Inorganic Chemistry

Article

pubs.acs.org/IC

The Effect of π Contacts between Metal Ions and Fluorophores on the Fluorescence of PET Sensors: Implications for Sensor Design for Cations and Anions

Joseph W. Nugent,[†] Hyunjung Lee,[†] Hee-Seung Lee,[†] Joseph H. Reibenspies,[§] and Robert D. Hancock*[,†]

[†]Department of Chemistry and Biochemistry, University of North Carolina Wilmington, Wilmington, North Carolina 28403, United States

[§]Department of Chemistry, Texas A&M University, College Station, Texas 77843, United States

Supporting Information

ABSTRACT: The idea that M···C π contacts between diamagnetic heavy metal ions such as Pb(II), Ag(I), Pd(II), or Hg(II) and the anthracenyl fluorophore of adpa ((**N**-(9-anthracenylmethyl)-**N**-(2-pyridinylmethyl)-2-pyridinemethanamine) are responsible for quenching the fluorescence of the complexes of these metal ions with adpa is explored crystallographically. The structures of $[Pb(adpa)(NO_3)_2]$ (**1**), $[Ag(adpa)NO_3]$ (**2**), $[Pd(adpa)NO_3]NO_3$ (**3**), $[Zn(adpa)(NO_3)_2]$ (**4**), and $[Cd(adpa)Br_2]$ (**5**) are reported. The π contacts with the fluorophore are for **1** are a Pb···C π contact of 3.178 Å; for **2**, an Ag···C π contact of 3.016 Å; and for **3**, a Pd···C π contact of 2.954 Å on the axial site of the Pd(II) ion. The Zn(II) ion in **4** has no Zn···C π contact, with the anthracenyl fluorophore rotated completely away from the Zn(II) ion. These structures confirm that in the Pb(II), Ag(I), and Pd(II) complexes of adpa, which experience strong quenching of fluorescence, there are strong M···C π contacts, as expected if it is the π contacts that quench fluorescence. In contrast, for the Zn(II) adpa complex, which forms no π contact, there is a strong increase in fluorescence intensity. The structure of **5** shows a long Cd···C π contact at 3.369 Å, in contrast to a previously reported structure with two coordinated nitrates where the Cd···C π contact is 3.097 Å. The long Cd···C π contact in $[Cd(adpa)Br_2]$ suggests how coordination of Br^-, as well as other more covalently bound ligands such as Cl^-, SCN^-, and $S_2O_3^{2-}$, cause an increase in fluorescence intensity, reported for the Cd(II)adpa complex in 50% CH_3OH/H_2O. Coordination of covalently bound ligands to the Cd(II) weakens the Cd···C π contact and so enhances fluorescence, whereas more ionically bound ligands such as SO_4^{2-}, NO_3^-, or H_2O produce a strong Cd···C π contact and weakened fluorescence. Complexes of the Cd(II)/adpa type may form the basis for a new type of anion/small molecule sensor. The tendency of metal ions to form π contacts with aromatic groups is analyzed in terms of the frequency of occurrence of π contacted structures in the literature, as well as by DFT calculations on the adpa complexes.

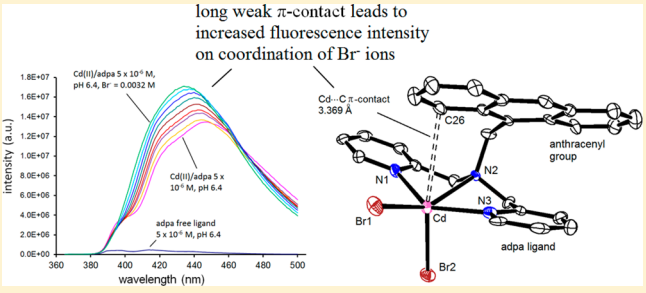

INTRODUCTION

The development of fluorescent sensors for both cations and anions is of considerable importance, as evidenced by a selection of reviews.[1−10] The development of "turn-on" sensors, which show an increase in fluorescence intensity in the presence of the target to be sensed, is generally more desirable than "turn-off" sensors, where fluorescence intensity decreases.[9] Of particular interest are metal-ion related factors that appear to control the intensity of the PET (photoinduced electron transfer) effect. Of importance in this work is the heavy atom effect,[10,11] where diamagnetic heavy metal ions such as Ag(I), Hg(II), Pb(II), and Bi(III) cause a large decrease in fluorescence intensity, which has been proposed to be associated with the large spin orbit coupling constants (ζ) present in metal ions of high atomic weight. It has been pointed out[11] that diamagnetic metal ions of high atomic weight such as La(III) and Lu(III), with large ζ values, produce large CHEF (chelation enhanced fluorescence) effects, leading to the suggestion that covalence in the M−L (metal−ligand) bond is necessary to cause fluorescence quenching by heavy metal ions. Recent DFT calculations have suggested[12] that significant covalence in a π contact from the targeted metal ion to the fluorophore may be sufficient to induce a fluorescence quenching effect. There are two types of fluorescent metal ion sensors (Scheme 1):[10] (a) sensors such as dqpma[13] or Zinquin[14] (see Figure 1 for ligand abbreviations) where the fluorophore has heteroatoms that coordinate to the metal ion and cause a CHEF (chelation-enhanced fluorescence) effect and (b) PET sensors with tethered fluorophores, such as on the adpa complex,[12] where the fluorophore has no heteroatoms capable of coordinating to the metal ion. Both types can show

Received: April 25, 2014
Published: August 21, 2014

   dx.doi.org/10.1021/ic5008632 | Inorg. Chem. 2014, 53, 9014−9026

Scheme 1. (a) Coordinated Fluorophores As Involved in the CHEF Effect and (b) Tethered Fluorophores As Are Present in PET Sensors

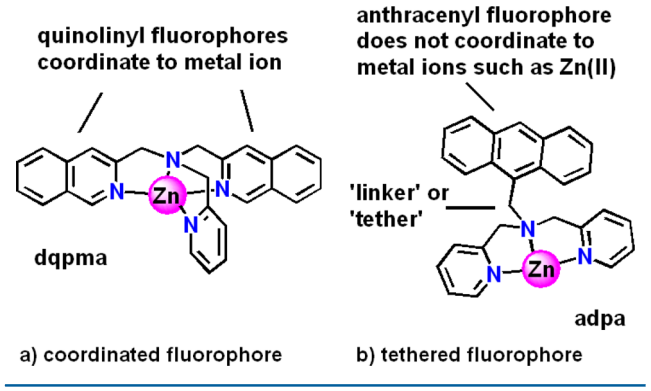

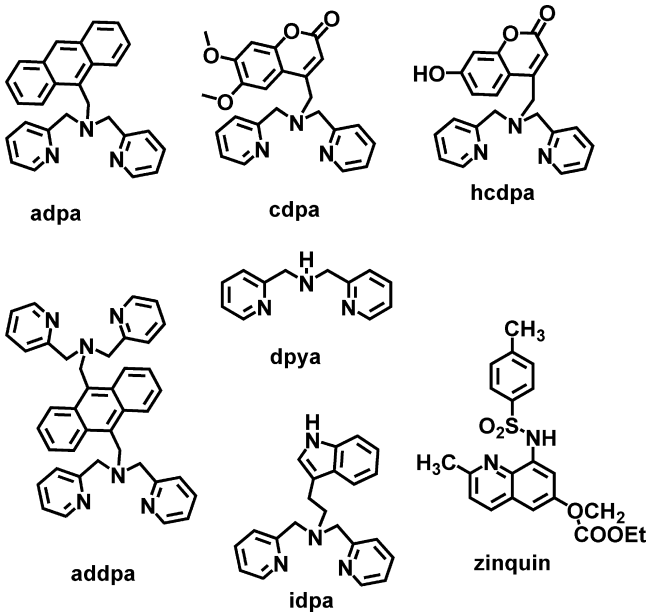

Figure 1. Some fluorescent sensors and ligands discussed in this paper.

quenching in the presence of diamagnetic heavy metal ions such as Hg(II). It is not obvious that Hg(II) can form a covalent bond to the anthracenyl fluorophore of adpa, if it is the case that such a bond is necessary to quench the fluorescence. The observation of π contacts in the case of adpa complexes does not mean that all quenching by diamagnetic heavy metal ions with all types of PET sensors needs to involve a π contact. For example, lengthening of M–L bonds due to steric or electronic effects can also restore the PET effect and so lead to quenching of fluorescence.[12] A further important factor is the role of intermolecular and intramolecular solvent-dependent hydrogen bonding in quenching fluorescence.[8] It is also possible that simple longer distance overlap between the orbitals of the metal ion and the orbitals of the π system of the fluorophore[10] might be sufficient to quench fluorescence in other sensors. One would hope that all of these effects could be woven into a coherent theory of fluorescence quenching.

In recent studies,[12] it was shown crystallographically that Hg(II) forms a strong π contact with the anthracenyl fluorophore of adpa, the π contact which was proposed, as supported by TDDFT (time-dependent DFT) calculations, to form a covalent contact with the fluorophore so as to quench the fluorescence. The DFT calculations suggested that in the non-π contacted fluorophore, the light-emitting $\pi^*-\pi$ transition occurs entirely within the π system of the fluorophore, but with a π contacted Hg(II) present, the LUMO and LUMO +1 orbitals of the anthracenyl group have significant Hg character, and the potentially emissive $S_1 \rightarrow S_0$ transition has significant charge transfer character and is weakened. In more recent work, crystal structures of Cd(II) complexes[15] of adpa showed both π-contacted and non-π-contacted forms, depending on the anions coordinated to the Cd(II) ion. With the ionically bound NO_3^- anion, a short Cd···C π contact of 3.018 Å was found crystallographically. Particularly interesting was the fact that anions such as Cl^-, Br^-, or $S_2O_3^{2-}$ caused increases in fluorescence intensity with increasing concentration in solution, suggesting the use of the Cd(II)/adpa complex as an anion sensor. Crystal structures showed that with two chlorides coordinated to the Cd(II)/adpa complex, the Cd···C π contact was lengthened to 3.282 Å, indicating a weakened π contact that might account for the increase in fluorescence intensity of the Cd(II)/adpa complex. With three chlorides coordinated to the Cd(II), the π contact was ruptured completely, which could then account for the increased fluorescence intensity of the Cd(II)/adpa complex in chloride solution.

Examination of structures in the CSD[16] (Cambridge Structural Database) shows that π contacts are exceedingly common with a wide range of metal ions, as discussed in some papers and reviews.[17] One has, of course, to be careful when relating crystal structures to solution structures, since these may not be the same. Thus, the solid state structures of Cu(II) with adpa both[12,18] show an anthracenyl fluorophore that is rotated away from the Cu(II), with no π contact. This is particularly important to the second type of metal ion property that leads to strong quenching of fluorescence, with implications for sensor design, namely the presence of unpaired electrons in either d-block metal ions such as Cu(II) or Fe(III), or f-block metal ions such as Nd(III) or Gd(III). The structures of Cu(II) with adpa[12,18] suggest that no π contact is necessary for Cu(II) to quench the fluorescence of adpa and that the electron is able to travel some distance to exert the redox mechanism that is thought to cause quenching by paramagnetic metal ions. However, a structure reported[19] for the Cu(II) complex of cdpa, similar to adpa except that a coumarin rather than an anthracenyl fluorophore is present, shows a short π contact of 2.987 Å. It may be that, as suggested for Cd(II),[15,20] there is an equilbrium in solution between π-contacted and non-π-contacted forms of the complex, and that for the Cu(II) complex the presence of the π contacted form facilitates electron transfer, and so the quenching of fluorescence. Design of turn-on sensors for Cu(II) could then incorporate steric prevention of such π contacts. It should be pointed out, however, that redox quenching mechanisms for metal ions such as Ni(II) or Ln(III) ions must also involve electron transfer without π contacts, since such metal ions almost never form π contacts in complexes that might relate to sensors in aqueous solution, as discussed below.

In this paper, the possible formation of π contacts with adpa by Ag(I), Zn(II) Pb(II), Pd(II), and Cd(II) (bromide anions) is investigated crystallographically, which is related to the effect that these metal ions have on the fluorescence of adpa. Also reported are the effects of some anions on the fluorescence intensity of the Cd(II)/adpa complex, which suggests possible

dx.doi.org/10.1021/ic5008632 | Inorg. Chem. 2014, 53, 9014–9026

Table 1. Crystal Data and Details of Structure Refinement for $[Pb(adpa)(NO_3)_2]$ (1), $[Ag(adpa)NO_3]\cdot CH_3OH$ (2), $[Pd(adpa)NO_3]NO_3$ (3), $[Zn(adpa)(NO_3)_2]$ (4), and $[Cd(adpa)Br_2]$ (5)

	1	2	3	4	5
empirical formula	$C_{27}H_{23}N_5O_6Pb$	$C_{28}H_{27}AgN_4O_4$	$C_{27}H_{23}N_5O_6Pd$	$C_{27}H_{23}N_5O_6Zn$	$C_{27}H_{23}N_3CdBr_2$
fw	720.69	591.40	619.90	578.87	661.70
temp (K)	150(2)	110(2)	110(2)	110(2)	110(2)
wavelength (Å)	0.71073	0.71073	0.71073	0.71073	0.71073
cryst syst	monoclinic	monoclinic	triclinic	monoclinic	monoclinic
space group	$P2_1/c$	$P2_1/n$	$P\bar{1}$	$P2_1/c$	$P2_1/n$
unit cell dimensions					
a (Å)	10.4892(16)	10.7630(19)	7.5393(3)	15.1541(7)	13.6309(10)
b (Å)	15.840(3)	17.963(3)	10.1956(4)	12.0215(5)	8.8751(5)
c (Å)	16.031(5)	13.180(2)	16.2874(6)	15.4235(7)	20.8287(14)
α (deg)	90	90	84.040(3)	90	90
β (deg)	109.070(12)	104.991(8)	81.944(3)	118.795(2)	103.443(5)
γ (deg)	90	90	75.147(3)	90	90
vol (Å^3)	2517.4(10)	2461.5(7)	1195.18(8)	2462.34(19)	2450.7(3)
Z	4	4	2	4	4
final R indices $[I > 2\sigma(I)]$	R_1 = 0.0210	R_1 = 0.0390	R_1 = 0.0292	R_1 = 0.0400	R_1 = 0.0422
	wR_2 = 0.0449	wR_2 = 0.0711	wR_2 = 0.0782	wR_2 = 0.0424	wR_2 = 0.0655
R indices (all data)	R_1 = 0.0292	R_1 = 0.0783	R_1 = 0.0343	R_1 = 0.1125	R_1 = 0.0944
	wR_2 = 0.0470	wR_2 = 0.0927	wR_2 = 0.0972	wR_2 = 0.1150	wR_2 = 0.1011

future directions in the designs of fluorescent sensors for anions and small molecules.

EXPERIMENTAL SECTION

Materials. The ligand adpa was synthesized following a literature method.[21] The metal salts $Pb(NO_3)_2$, $Pd(NO_3)_2\cdot H_2O$, $AgNO_3$, $Zn(NO_3)_2\cdot 6H_2O$, $CdBr_2$, and metal perchlorates were obtained from VWR or Strem in ≥99% purity and used as received. All solutions were made up in deionized water (Milli-Q, Waters Corp.) of >18 MΩ cm^{-1} resistivity, plus HPLC grade methanol from Merck. Solutions for mass spectrometry were prepared in LC/MS grade methanol and DMSO.

Elemental Analyses. The C and N elemental compositions were measured with a CE Elantech model NC 2100CHN analyzer.[22] This offers the advantage that individual crystals can be selected for in-house analysis, although analyses for H are not obtained. This is not considered to be a drawback, as the H analyses are not particularly informative, being rather small percentages that show relatively little variation within one type of complex such as adpa complexes.

Mass Spectral Measurements. The mass spectral data were acquired on a Bruker MicroQ-TOF II mass spectrometer equipped with an electrospray ionization (ESI) interface operated in the positive mode. The stock solution was prepared in DMSO and then diluted down with methanol with 0.1% formic acid to a DMSO/methanol ratio of 1:4. The process was repeated with nonacidified methanol to a DMSO/methanol ratio of 1:3.

*Synthesis of $[Pb(adpa)(NO_3)_2]$ (**1**).* One equivalent of adpa (35.0 mg, 0.09 mmol) was dissolved in methanol (3 mL) and added to a solution of one equivalent of $Pb(NO_3)_2$ (29.8 mg, 0.09 mmol) in methanol (3 mL) in a 20 mL sample vial. The vial containing the resulting solution was placed standing upright in a jar with a lid, containing diethyl ether to a depth of about 5 mm, and the jar was tightly closed. Diffusion of diethyl ether vapor into the solution resulted in deposition of pale-yellow crystals over a period of a few days. Yield, 25.7 mg = 39.6%. IR spectrum, more intense bands (cm^{-1}): 3048, 2395, 1570, 1433, 1383, 1050, 833, 764. Elemental analysis calcd. for $C_{27}H_{23}PbN_5O_6$: C, 45.00%; N, 9.72%. Found: C, 44.90%; N, 9.54%.

*Synthesis of $[Ag(adpa)NO_3]$ (**2**).* One equivalent of adpa (35.0 mg, 0.09 mmol) was dissolved in methanol (2.5 mL) and added to a solution of 1 equiv of $AgNO_3$ (15.2 mg, 0.09 mmol) in methanol (1 mL) in a 20 mL sample vial. Diffusion of diethyl ether vapor in a sealed container was used for crystal growth as described for the Pb(II) crystals. The solution was filtered off under a vacuum, and the crystals were air-dried. Yield, 26.3 mg = 49.7%. IR spectrum more intense bands (cm^{-1}): 3050, 2847, 1589, 1474, 1378, 1096, 767, 733. Elemental analysis calcd. for $C_{28}H_{27}AgN_4O_4$: C, 57.16%; N, 9.52%. Found: C, 57.45%; N, 9.55%.

*Synthesis of $[Pd(adpa)NO_3]NO_3$ (**3**).* One equivalent of adpa (35.0 mg, 0.09 mmol) was dissolved in methanol (4 mL) and added to a solution of 1 equiv of $Pd(NO_3)_2\cdot H_2O$ (20.7 mg, 0.09 mmol) in methanol (3 mL) in a 20 mL sample vial. Diffusion of diethyl ether vapor in a sealed container, as described for the Pb(II) crystals, did not result in deposition of crystals. The lid was loosened to allow the solution to slowly evaporate. This resulted in the formation of very few small pale-orange crystals after approximately one month. The solution was filtered off under a vacuum, and the crystals were air-dried. The yield was very low (~5%) and did not permit a satisfactory elemental analysis. The mass spectral data supported the presence of the above complex in the crystals obtained: ESI-MS m/z = 390 [adpa + H]$^+$; m/z = 638 [adpa + Pd + 2NO$_3$ + H$_2$O + H]$^+$. IR spectrum, more intense bands (cm^{-1}): 3029, 1679, 1610, 1380, 1306, 1286, 1171, 819, 693.

*Synthesis of $[Zn(adpa)(NO_3)_2]$(**4**).* One equivalent of adpa (35.0 mg, 0.09 mmol) was dissolved in methanol (4 mL) and added to a solution of 1 equiv of $Zn(NO_3)_2 6H_2O$ (26.7 mg, 0.09 mmol) in methanol (3 mL) in a 20 mL sample vial. Diffusion of diethyl ether vapor into the solutions, as described for the Pb(II) complex, resulted in deposition of pale-yellow crystals over a period of a few hours. The solution was filtered off under a vacuum, and the crystals were air-dried. Yield, 25.0 mg = 48.0%. IR spectrum, more intense bands (cm^{-1}): 2925, 1659, 1606, 1378, 1292, 1100, 1024, 730. Elemental analysis calcd. for $C_{27}H_{23}ZnN_5O_6$: C, 56.02%; N, 12.10%. Found: C, 56.36%; N, 11.89%.

*Synthesis of $[Cd(adpa)Br_2]$ (**5**).* One equivalent of adpa (35.0 mg, 0.09 mmol) was dissolved in methanol (3 mL) and added to a solution of 1 equiv of $CdBr_2\cdot 4H_2O$ (30.9 mg, 0.09 mmol) in methanol (5 mL) in a 20 mL sample vial. Diffusion of diethyl ether vapor in a sealed container was used for crystal growth as described for the Pb(II) crystals, which resulted in deposition of needle-like pale-yellow crystals in a matter of minutes. The solution was filtered off under a vacuum and the crystals were air-dried. Yield, 21.8 mg = 38.7%. IR spectrum more intense bands (cm^{-1}): 3053, 2919, 1602, 1442, 1296, 1018, 762, 730. Elemental analysis calcd. for $C_{27}H_{23}CdBr_2N_3$: C, 49.01%; N, 6.35%. Found: C, 49.03%; N, 6.09%.

Molecular Structure Determination. A BRUKER D8-GADDS X-ray (three-circle) diffractometer was employed for crystal screening, unit cell determination, and data collection. The structures were solved

dx.doi.org/10.1021/ic5008632 | Inorg. Chem. 2014, 53, 9014−9026

Table 2. Selection of Bond Lengths and Angles for $[Pb(adpa)(NO_3)_2]$ (1)

bond lengths (Å)					
Pb(1)–N(1)	2.4474(15)	Pb(1)–O(4)	2.5181(15)	Pb(1)–N(3)	2.6093(16)
Pb(1)–N(2)	2.6406(14)	Pb(1)–O(3)	2.7017(15)		
bond angles (deg)					
N(1)–Pb(1)–O(4)	76.44(5)	N(1)–Pb(1)–N(3)	98.06(5)		
O(4)–Pb(1)–N(3)	83.21(5)	N(1)–Pb(1)–N(2)	66.21(4)		
O(4)–Pb(1)–N(2)	125.61(5)	N(3)–Pb(1)–N(2)	65.42(4)		
N(1)–Pb(1)–O(3)	73.60(5)	O(4)–Pb(1)–O(3)	79.32(5)		
N(3)–Pb(1)–O(3)	161.98(4)	N(2)–Pb(1)–O(3)	122.44(4)		

by direct methods and refined to convergence.[23] Details of the structure determination are given in Table 1, and crystal coordinates and details of the structure determination of **1**–**5** have been deposited with the CSD (Cambridge Structural Database).[16] A selection of bond lengths and angles for **1** to **5** are given in Tables 2–6. The structures of **1**–**5** are shown in Figures 2–6.

Table 3. Selection of Bond Lengths and Angles for $[Ag(adpa)NO_3]$ (2)

bond lengths (Å)					
Ag(1)···Ag(1)′ 3.2659(6)	Ag(1)–O(1)	2.7472(19)	Ag(1)–O(2)	2.679(2)	
Ag(1)–N(1) 2.2796(13)	Ag(1)–N(2)	2.6227(13)	Ag(1)–N(3)	2.3007(13)	
bond angles (deg)					
O(2)–Ag(1)–O(1)	46.34(4)	N(1)–Ag(1)–O(1)	83.57(5)		
N(1)–Ag(1)–O(2)	129.69(4)	N(1)–Ag(1)–N(2)	71.49(4)		
N(1)–Ag(1)–N(3)	143.35(5)	N(2)–Ag(1)–O(1)	146.61(4)		
N(2)–Ag(1)–O(2)	148.33(4)	N(3)–Ag(1)–O(1)	131.78(5)		
N(3)–Ag(1)–O(2)	85.60(4)	N(3)–Ag(1)–N(2)	72.27(4)		

Table 4. Selection of Bond Lengths and Angles for $[Pd(adpa)NO_3]NO_3$ (3)

bond lengths (Å)					
Pd(1)–O(1)	2.055(3)	Pd(1)–N(1)	2.012(4)	Pd(1)–N(2)	2.006(3)
Pd(1)–N(3)	2.019(3)				
bond angles (deg)					
N(1)–Pd(1)–O(1)	93.88(13)	N(1)–Pd(1)–N(3)	166.25(14)		
N(2)–Pd(1)–O(1)	173.34(13)	N(2)–Pd(1)–N(1)	83.74(14)		
N(2)–Pd(1)–N(3)	84.66(14)	N(3)–Pd(1)–O(1)	98.44(13)1		

Table 6. Selection of Bond Lengths and Angles for $[Cd(adpa)Br_2]$ (5)

bond lengths (Å)					
Cd(1)–Br(1)	2.5501(9)	Cd(1)–Br(2)	2.6264(9)	Cd(1)–N(1)	2.309(6)
Cd(1)–N(2)	2.491(5)	Cd(1)–N(3)	2.287(6)		
bond angles (deg)					
Br(1)–Cd(1)–Br(2)	112.55(3)	N(1)–Cd(1)–Br(1)	102.25(16)		
N(1)–Cd(1)–Br(2)	98.80(15)	N(1)–Cd(1)–N(2)	70.6(2)		
N(2)–Cd(1)–Br(1)	152.21(12)	N(2)–Cd(1)–Br(2)	95.20(13)		
N(3)–Cd(1)–Br(1)	104.65(16)	N(3)–Cd(1)–Br(2)	97.42(15)		
N(3)–Cd(1)–N(1)	140.13(19)	N(3)–Cd(1)–N(2)	71.8(2)		

Fluorescence Measurements. Excitation–emission matrix (EEM) fluorescence properties were determined on a Jobin Yvon SPEX Fluoromax-3 scanning fluorometer equipped with a 150 W Xe arc lamp and a R928P detector. The instrument was configured to collect the signal in ratio mode with a dark offset using 5 nm bandpasses on both the excitation and emission monochromators. The EEMs were created by concatenating emission spectra measured every 5 nm from 250 to 500 nm at 51 separate excitation wavelengths. Scans were corrected for instrument configuration using factory supplied correction factors. Post processing of scans was performed using the FluorEssence program.[24] The software eliminates Rayleigh and Raman scattering peaks by excising portions (±10–15 nm FW) of each scan centered on the respective scatter peak. The excised data are replaced using three-dimensional interpolation of the remaining data according to the Delaunay triangulation method and constraining the interpolation such that all nonexcised data are retained. Following removal of scatter peaks, data were normalized to a daily determined water Raman intensity (275ex/303em, 5 nm bandpasses). Replicate scans were generally within 5% agreement in terms of intensity and within bandpass resolution in terms of peak location. The fluorescence of the adpa solutions was recorded in 50% MeOH/water.

Table 5. Selection of Bond Lengths and Angles for $[Zn(adpa)(NO_3)_2]$ (4)

bond lengths (Å)					
Zn(1)–N(1)	2.0618(17)	Zn(1)–N(3)	2.0699(18)	Zn(1)–O(4)	2.0918(15)
Zn(1)–O(1)	2.1585(15)	Zn(1)–N(2)	2.2703(18)	Zn(1)–O(3)	2.4148(16)
Zn(1)–O(6)	2.549(2)				
bond angles (deg)					
N(1)–Zn(1)–N(3)	157.02(8)	N(1)–Zn(1)–O(4)	102.27(6)		
N(3)–Zn(1)–O(4)	97.12(7)	N(1)–Zn(1)–O(1)	100.79(6)		
N(3)–Zn(1)–O(1)	94.49(6)	O(4)–Zn(1)–O(1)	80.25(6)		
N(1)–Zn(1)–N(2)	78.94(6)	N(3)–Zn(1)–N(2)	78.24(6)		
O(4)–Zn(1)–N(2)	140.80(6)	O(1)–Zn(1)–N(2)	138.60(6)		
N(1)–Zn(1)–O(3)	90.81(6)	N(3)–Zn(1)–O(3)	83.60(6)		
O(4)–Zn(1)–O(3)	136.02(5)	O(1)–Zn(1)–O(3)	55.97(5)		
N(2)–Zn(1)–O(3)	82.65(5)				

dx.doi.org/10.1021/ic5008632 | Inorg. Chem. 2014, 53, 9014–9026

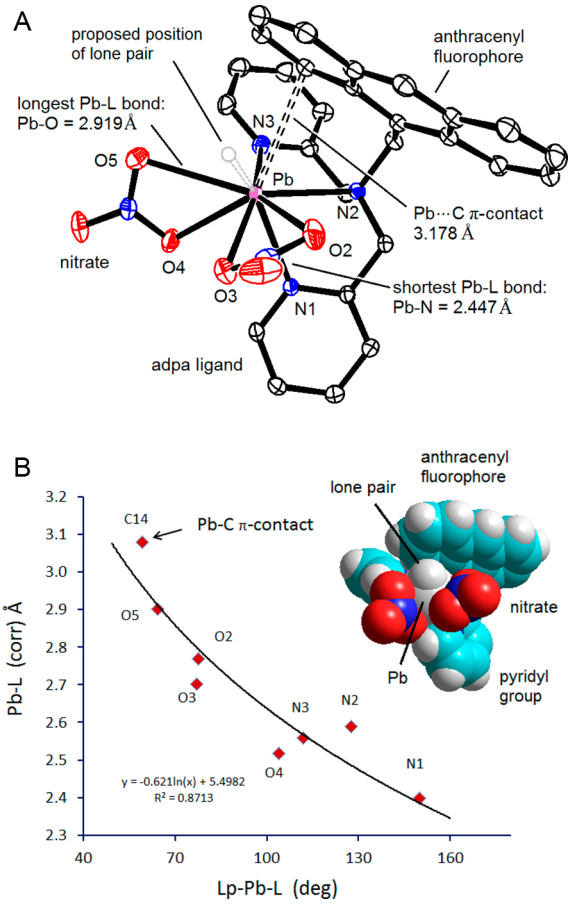

Figure 2. (a) Structure of $[Pb(adpa)(NO_3)_2]$ (**1**), showing the Pb···C π contact of 3.178 Å. The position of the lone pair on Pb, estimated as described in the text (see Figure 2b), is shown, occupying an apparent gap in the coordination geometry of the Pb(II). Hydrogen atoms are excluded for clarity. Thermal ellipsoids are drawn at the 50% confidence level. Drawing made with ORTEP.[32] (b) Relationship between Pb–L (L = ligand) bond length, and the Lp–Pb–L angle (Lp = lone pair), in the structure of $[Pb(adpa)(NO_3)_2]$ (**1**). The Pb–L bond lengths are corrected for differences in covalent radii of the donor atoms, as discussed in the text. The proposed position of the lone pair on the Pb is adjusted so as to optimize the fit of the curve of the Pb–L bond lengths to the resulting Lp–Pb–L angles. Also shown in the diagram is a space-filling drawing of the $[Pb(adpa)(NO_3)_2]$ complex, showing the position of the lone pair as suggested by the analysis undertaken in this diagram.

Density Functional Theory (DFT) Calculations. All DFT/TDDFT calculations reported in this work were carried out with the *ab initio* quantum chemistry package GAMESS.[25] Geometry optimization of the M^{II}/adpa (M = Ca, Zn, Cd, Hg, and Pb) complexes was performed within the framework of Kohn–Sham DFT with B3LYP exchange-correlation functional.[26,27] The SV(P) basis set[28] was used for the main group elements, whereas the Lanl2DZ[29−31] effective core potential was employed for the metal ions. For the complexes with the anthracenyl fluorophore turned away from the metal, three water molecules are coordinated to the metal ion (two axial and one equatorial positions of octahedral complex). On the other hand, the complexes with a π contact have two water molecules (one axial and one equatorial) coordinated to the metal ion.

RESULTS AND DISCUSSION

Structure of $[Pb(adpa)(NO_3)_2]$ (1). The structure of **1** (Figure 2a)[32] shows typical coordination geometry for Pb(II), with an apparent gap in the coordination sphere which is the

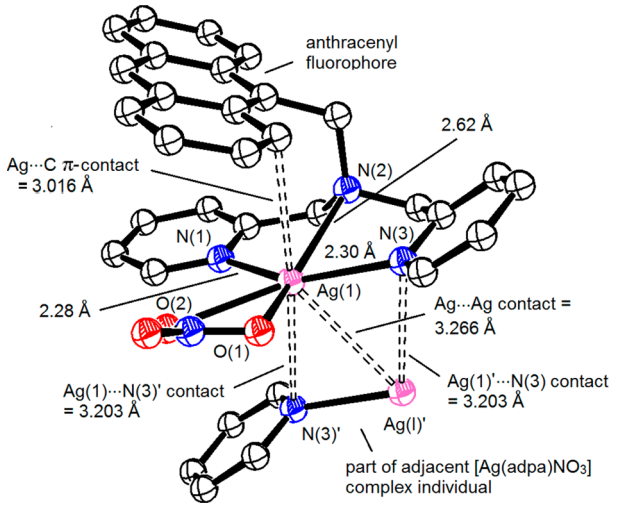

Figure 3. Structure of the $[Ag(adpa)NO_3]$ complex from **2**, showing the Ag···C π contact of 3.016 Å. Also shown are the Ag···Ag contact to Ag(I)′ from an adjacent $[Ag(adpa)NO_3]$ complex and the short Ag(1)–N(3) contacts between the complexes. Hydrogen atoms are excluded for clarity. Drawing made with ORTEP.[32]

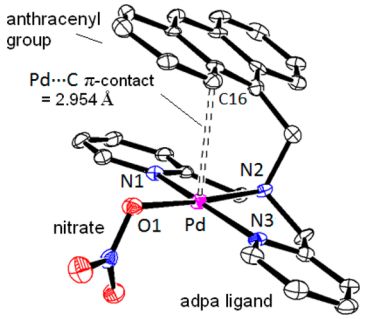

Figure 4. Structure of the $[Pd(adpa)NO_3]^+$ complex cation from **3**, showing the Pd···C π–contact of 2.954 Å. Hydrogen atoms are excluded for clarity. Thermal ellipsoids drawn at the 50% confidence level. Drawing made with ORTEP.[32]

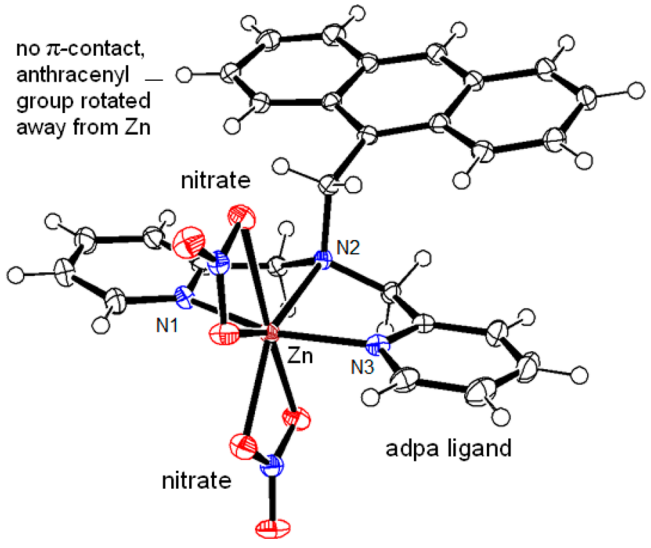

Figure 5. Structure of the $[Zn(adpa)(NO_3)_2]$ complex from **4**, showing the absence of a Zn···C π–contact. Thermal ellipsoids drawn at the 50% confidence level. Drawing made with ORTEP.[32]

dx.doi.org/10.1021/ic5008632 | Inorg. Chem. 2014, 53, 9014–9026

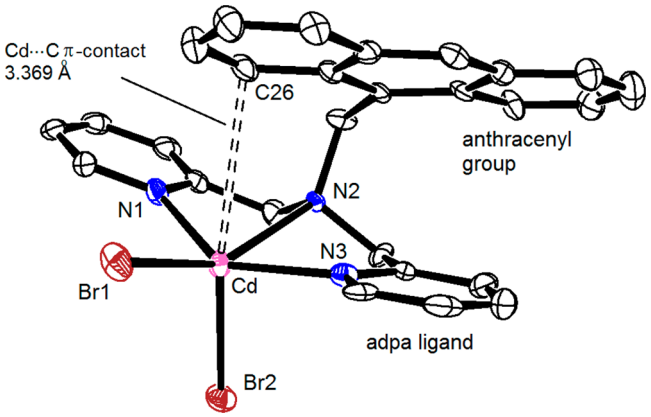

Figure 6. Structure of the $[Cd(adpa)Br_2]$ complex from **5**, showing the long Cd···C π contact of 3.369 Å. Hydrogen atoms are excluded for clarity. Thermal ellipsoids drawn at the 50% confidence level. Drawing made with ORTEP.[32]

supposed site of the lone pair (Lp) on the Pb(II) ion.[33−37] There are short M−L (metal−ligand) bonds on the side of the Pb atom away from the proposed site of the lone pair, with the M−L bonds growing progressively longer as one proceeds toward the site of the lone pair.[33−37] In the case of the Pb(II) in structure **1**, Pb−N(1) from a pyridyl group (2.447 Å) and Pb−O(4) from a nitrate (2.518 Å) are the shortest bond lengths (Table 2). The remaining two Pb−N bonds are longer at 2.609 and 2.641 Å. The lone pair is thought to be located in the vicinity of the longest bonds in the structure, in this case PbO(5) (2.919 Å). The proposed position of the lone pair in Figure 2a was obtained as suggested previously[37] from a plot of the Lp−Pb−L angles vs the Pb−L lengths (Figure 2b). The Pb−L bond lengths are corrected for the greater covalent radius[38] of the N (0.71 Å) and C donor atoms (0.76 Å) as compared to the O donor atoms (0.66 Å) by subtracting 0.05 Å from the Pb−N lengths and 0.10 Å from the Pb···C length. The position of the lone pair is adjusted so as to produce the best fit to the curve of Pb−L length vs Lp−Pb−L angle. Such plots typically show that there is a fairly smooth increase in Pb−L bond length as the LpPbL angle gets smaller, i.e. as the donor atoms forming the bonds get closer to the site of the lone pair on Pb(II). The position of the lone pair is indicated in the space-filling drawing shown in Figure 2b. The latter shows how the analysis of Pb−L bond length vs Lp−Pb−L angle places the lone pair in exactly the gap that is present in the coordination sphere around the Pb. What is of interest in Figure 2b is that the Pb···C π contact is quite close to the site of the lone pair, and that the Pb···C distance is not greatly longer than would be expected from the relationship between Pb−L length and the LpPbL angle shown in Figure 2b.

The Pb(II) complex is the only structure of an adpa complex so far determined,[12,15] apart from the $[Cd(adpa)Cl_2]_2$ dimer,[15] where the adpa is coordinated in essentially a *fac* (facial) rather than a *mer* (meridional) fashion. This can be understood as arising from the need for at least one of the more covalently binding pyridyl N donors to occupy the favored site opposite the lone pair. If the adpa adopted a *mer* mode of coordination, this would force one of the two pyridyl groups to be coordinated very close to the lone pair, if the other pyridyl donor occupied the favored site opposite the lone pair. This would mean placing one of the two most covalently binding donor atoms close to the less-favored site near the lone pair.

It should be noted that, although a logarithmic relationship was used to generate a smooth curve to fit to the structural data in Figure 2b, there is no theoretical basis for choosing such a relationship, and a polynomial can give an equally good fit. It seems clear however from analysis[37] of several structures of Pb(II) complexes that the relationship is always curved, and not linear, and so a mathematical relationship was used in Figure 2b that would fit a curve to the experimental data.

Table 7. Number of π Contacts with Aromatic Carbon Atoms Found in the CSD[16] for a Selection of Metal Ions, the Average M···C π Contact Distance for Each Metal Ion, Plus Sum of van der Waals Radii for the Metal Plus Carbon (Estimated Radii in Parentheses)[a]

metal ion:	Cd(II)	Hg(II)	Ag(I)	Au(I)	Sn(II)	Pb(II)	Sb(III)	Bi(III)	Cu(II)[b]	Ni(II)[b]	Zn(II)[c]	Pd(II)[b]	Pt(II)[b]
no. π contacts[d]	29	365	1580	260	62	173	139	85	489	79	15	57	35
min. no. contacts[e]	1	1	3	2	3	1	1	1	2	1	2	3	3
average M···C (Å)	3.05	3.56[f]	3.47[f]	3.62[f]	3.56	3.50	3.44	3.50	3.31[f]	3.26	3.02	3.21	3.29
sum VdW radii[g]	3.28	(3.25)	(3.42)	(3.36)	3.87	3.72	(3.5)	(3.7)	(3.10)	3.33	3.09	3.33	3.45
metal ion	Li(I)	Na(I)	K(I)	Rb(I)	Cs(I)	Ga(I)	In(I)	Tl(I)	Mg(II)*	Ca(II)*	Sr(II)*	Ba(II)*	Al(III)*	La(III)*
no. π contacts[d]	131	307	1069	93	144	17	14	146	6	39	13	30	1	34
min. no. contacts[e]	3	3	3	3	3	3	3	3	3	3	3	3	3	3
average M···C (Å)	3.14	3.23	3.49	3.54	3.73	3.11	3.34	3.39	3.08	3.09	3.33	3.42	3.30	3.26
sum VdW radii[g]	3.52	3.97	4.45	(4.5)	(4.5)	(3.6)	(3.6)	3.63	3.66	3.42	(3.6)	(3.8)	(3.5)	(3.6)

[a]An asterisk indicates complexes are nearly all of the organometallic type not likely to be relevant to species in solution. [b]All on axial sites of square planar (Ni(II), Pd(II), Pt(II), Cu(II)) complexes or square pyramidal complexes (Cu(II)). [c]Mostly on axial sites of Zn porphyrins (eight examples) or low coordination number Zn aryl/alkyl compounds. [d]The criterion for a π contact is that the M···C nonbonded distance be less than the sum of the van der Waals radii of the metal plus that of the carbon atom (1.70 Å[41]). As discussed in the text, very short M···C contacts that are designated as actual M−C bonds by the CSD are excluded from this table, even though the metal ion has not displaced the H atom from the contacted carbon. In defining such contacts in a search, as discussed in the text, one has to exclude, for example, phenyl groups bonded to metals, that give short M···C distances to the *ortho* carbons, and the very numerous structures where metal ions contact aromatic rings approximately side-on. [e]The searches were conducted with "hits" being those where the metal ion lay more or less above the plane of the aromatic ring, and not side-on to it. This was achieved where necessary by requiring more than one M···C contact to the same ring (2 or 3 as indicated) shorter than the sum of the van der Waals radii. [f]For metal ions with distorted coordination spheres, the π contacts may occupy sites with longer M···C contacts than allowed by looking only at the sum of the van der Waals radii: for Ag(I), Hg(II), and Au(I), with long bonds at right angles to the two short bonds forming a linear arrangement, distances up to 3.8 Å were considered. For Cu(II) with its tetragonal distortion, distances up 3.6 Å were considered. [g]van der Waals radii (Å) from ref 41.

dx.doi.org/10.1021/ic5008632 | *Inorg. Chem.* 2014, 53, 9014−9026

What is of particular interest in the Pb(II)/adpa structure is why the Pb···C π contact should be located so near the position of the lone pair, and what this suggests about the nature of M···C π contacts in general.

Structure of [Ag(adpa)(NO_3)]·CH_3OH (2). The structure of **2** (Figure 3) shows typical coordination geometry for d^{10} metal ions such as Ag(I) or Hg(II). These d^{10} metal ions often show a preference for what can be regarded as linear coordination geometry, even when there are more than two donor atoms coordinated to the metal ion:[37,39] this is particularly true when two of the donor atoms can form more covalent M−L bonds than the other donor atoms. Typically, there are two short M−L bonds at roughly 180° to each other, with other bonds at roughly right angles to the two short bonds, with much longer M−L bond lengths.[36,37,39] Usually, the short M−L bonds (the "linear" coordination sites) involve the donor atoms capable of forming the most covalent bonds, while more ionically bound donor atoms occupy the long bonds at right angles to the two short bonds. Such an arrangement is found for Hg(II)/adpa complexes[12] and is found here also for the Ag(I)/adpa complex in Figure 3. As with the Hg(II)/adpa structure, the two bonds to the sp^2 hybridized N donors of the pyridyl groups, which presumably form the most covalent M−L bonds, occupy the approximately linear sites with short Ag−N bond lengths of Ag−N(1) = 2.280 Å and Ag−N(3) = 2.301 Å, with N(1)Ag−N(3) = 143.35°. The remaining bonds to the Ag(I) are much longer, with Ag−N(2) = 2.623 Å to the central sp^3 hybridized N donor of adpa, and AgO(1) = 2.747 Å and Ag−O(2) = 2.679 Å to the two O donors of the chelating nitrate. The Ag···C(14) π contact at 3.016 Å is quite short, typical of Ag complexes, and is best described as an η^1 bond, being placed directly above C(14). As seen in Table 7, Ag(I) shows in the CSD[16] a great number of π contacts with aromatic rings and further shows its affinity for aromatic rings by actually complexing benzene and other aromatic molecules in aqueous solution with measurable log K_1 values of about 0.5.[40] Because of the above distortion of the coordination sphere around Ag(I), a large number of Ag···C π contacts at distances longer (up to 3.8 Å) than the sum of the van der Waals radii[41] were included in Table 7, which shows numbers of structures containing π contacts found for a selection of metal ions as an indication of their tendency to form π contacts. This was also done for the similarly distorted Au(I) and Hg(II) π contacts, as well as for the tetragonally distorted Cu(II) complexes.The fact that Ag(I) forms a large number of π contacts is discussed below in terms of factors that control the tendency of metal ions to form π contacts.

The structure of **2** also shows that there is a short Ag···Ag contact distance of 3.266 Å between Ag atoms in adjacent [Ag(adpa)NO_3] individuals. Such "argentophilic" contacts are very common,[42] as shown by 1645 structures in the CSD,[16] showing such short Ag···Ag contacts, averaging 3.13 ± 0.18 Å. As seen in Figure 3, the short Ag···Ag contacts in **2** are accompanied by two short Ag···N contacts of 3.203 Å, making a trapezoid involving four Ag−N bonds or contacts, with the Ag···Ag contact occupying a diagonal across the trapezoid. Interestingly, this type of structure is not uncommon, with 20 structures in the CSD[16] showing this type of arrangement, with pyridyl groups coordinated to Ag(I) ions. The average Ag···Ag contact in these structures is 3.20 ± 0.13 Å, and the Ag···N contacts average 3.11 ± 0.11 Å. One sees in Figure 3 that the pyridyl group containing N(3) is rotated so as to direct the presumed position of the lone pair on N(3) to lie between the two silver atoms. The nature of the long Ag···N contacts is not clear, but it is possible that they represent Ag···N π contacts. Ag···C π contacts with pyridines are quite common: some 442 structures[16] yield average Ag···C π contacts with pyridines of 3.29 Å, not too different from the Ag···N contacts with pyridines of 3.11 Å once the larger van der Waals radius[41] of C (1.70 Å) than N (1.55 Å) is taken into account.

Not included in Table 7 are the 46 structures[16] for Ag(I) where the Ag···C π contacts occupy the favored "linear" coordination sites with the Ag(I) and are very short: these short contacts appear also quite often to be part of a trigonal planar, or tetrahedral, and not linear, arrangement of short bonds. These short Ag···C contacts, which average 2.495 ± 0.072 Å, are designated by the CSD search engine to be bonds rather than contacts, even though the contacted C is not deprotonated. These structures typically involve aromatics π contacted with the Ag(I) in an η^1 or η^2 mode, with less covalently binding donor groups such as sulfonic acids binding on the less favored remaining sites, with considerably longer Ag−O bonds. Hg(II) forms seven similar structures,[16] with η^1 Hg−C bonds to nondeprotonated aromatic carbons averaging 2.396 ± 0.0103 Å. A search of the CSD yields 167 structures with π contacts short enough to qualify as bonds with a wide variety of metal ions, with Ag(I) by far the most common. Cu(I) forms seven such structures,[16] with short Cu−C bonds averaging 2.306 ± 0.186 Å. Pd(II) forms 50 such structures where a "C=C" bond from an aromatic ring occupies an in-plane coordination site, much as ethylene groups do in numerous Pd(II) complexes, with Pd−C bonds averaging 2.307 ± 0.106 Å. Cu(II) and Cd(II) do not appear to form such bonds, while other metal ions such as Zn(II) (one example, Zn−C = 2.525 Å) or Li(I) (nine examples, Li−C = 2.50 ± 0.12 Å) form only a few examples, typically in sterically crowded organometallic environments with the metals having low coordination numbers.

Structure of [Pd(adpa)NO_3]NO_3 (3). The structure of **3** is seen in Figure 4, and bond lengths and angles of interest are shown in Table 4. The Pd has typical coordination geometry for a low-spin d^8 metal ion, with square-planar geometry, except for a π contact on the axial site of the Pd(II) with a short Pd···C distance of 2.954 Å. The formation of a fifth M−L bond is not unusual for low-spin Pd(II) complexes: a search of the CSD[16] reveals 84 five-coordinate Pd(II) complexes, excluding those where the axial coordination site is occupied by another metal. Of these, the vast majority have a square pyramidal structure with a long bond to the donor atom occupying the axial site, typically about 0.5 Å longer than similar bonds in the plane. Only 10 of these five coordinate Pd(II) complexes are best described as trigonal bipyramidal: these mostly involve tridentate or tripodal phosphine ligands that appear to force the geometry on the metal ion. The Pd(II)/adpa complex appears to have quite usual geometry for a five-coordinate Pd(II) complex, if it can be regarded as such, and raises the interesting question of what type of bonding the PdC π contact represents.

Structure of [Zn(adpa)(NO_3)$_2$] (4). The structure of **4** is seen in Figure 5, and bond lengths and angles of interest are shown in Table 5. The Zn(II) is effectively 7 coordinate, with the three N donors from adpa bonding to the Zn(II), as well as both of the nitrates chelated to the Zn(II). As happens so commonly,[16] the nitrate with its small "bite" distance (distance between the chelating donor atoms) is able to raise the coordination number of the Zn(II) above its most common

dx.doi.org/10.1021/ic5008632 | Inorg. Chem. 2014, 53, 9014−9026

value of 6. The Zn(II)/adpa complex has the anthracenyl group completely rotated away from the Zn(II) ion, and so no π contact is present. A similar complex of Zn(II) with the ligand addpa (Figure 1), which has two dpya groups attached to it, has two chlorides coordinated to each of the two Zn(II) ions bound to it.[43] The Zn(II) ions in the complex with addpa are only five-coordinate and square pyramidal, and it is of interest to note that the Zn(II) ions are placed somewhat over the anthracenyl group, although the Zn···C distance at 3.40 Å is perhaps too long to be considered a π contact, considering that the sum of the van der Waals radii of Zn and C is 3.09 Å.[41] As would be expected from this very long Zn···C contact, addpa shows a strong increase in fluorescence intensity on coordination of Zn(II) ions, while Cu(II) and Ni(II), as would be expected from a redox mechanism, show strong quenching.[43]

Structure of [Cd(adpa)Br$_2$] (5). The structure of **5** is seen in Figure 6, and bond lengths and angles of interest are shown in Table 6. Unlike the Cd(II)/adpa complex with two chlorides in the place of bromides,[15] **5** does not have dimers present with bromide bridges. The Cd(II) ion in **5** appears to be 5-coordinate, with three Cd−N bonds to the N donors of the adpa ligand, and two Cd−Br bonds. The Cd···C contact distance is 3.369 Å, perhaps too long to be regarded as a π contact, noting that the sum of the van der Waals radii of Cd and C is 3.28 Å.[41] One can see in the structures of Cd(II)/adpa complexes where the coordinated anions are NO_3^-, Cl^-, and Br^- that the Cd···C contacts become longer as the potential for covalent bonding of the coordinated anions becomes stronger, as suggested by decreasing electronegativity of the donor atoms. Thus, with two of each of the following anions coordinated to Cd(II) in its adpa complex, the Cd···C contact lengths are NO_3^-, 3.018 Å;[15] Cl^-, 3.282 Å;[15] and Br^-, 3.369 Å. These Cd···C distances parallel what happens with Hg(II)/adpa complexes,[12] where the Hg···C contact becomes longer as the coordinated anion is changed from Cl^- to Br^-.

An important point about the structure of the Hg(II)/adpa complexes is that the Hg−N bond to the central sp^3 hybridized N becomes longer as the Hg−L bonding to the coordinated halide ions becomes more covalent. The PET (photoinduced electron transfer) effect that quenches the fluorescence of the free adpa ligand leads to increased fluorescence intensity when this N donor is coordinated to a metal or proton. The PET effect quenches fluorescence because an electron falls from the lone pair of the noncoordinated N donor into the gap in the π-system of the fluorophore in its excited state. The increase in fluorescence intensity occurs because the coordinated M^{n+} or H^+ lowers the energy of the lone pair on the N donor below the energy of the π-system of the fluorophore, so removing the PET effect.

When such M−N bonds become too long, the energy of the lone pair on the N donor may not be lowered sufficiently, and the PET effect may still operate, leading to a weak or nonexistent CHEF effect.[12,44−49] One sees in (Table 6) that the Cd−N(2) bond to the central sp^3 hybridized N donor of the adpa ligand in **5** is normal in length: with the following anions coordinated to Cd(II)/adpa, the Cd−N(2) bond lengths to the sp^3 hybridized N are NO_3^-, 2.457 Å; Cl^-, 2.476 Å; and Br^- 2.491 Å. This modest increase in Cd−N(2) bond length as the covalence of the Cd−L bond to the coordinated anions increases can be compared with the corresponding Hg−N bonds to the central N of adpa: NO_3^-, 2.51 Å (DFT calculation); Cl^-, 2.603 Å; Br^-, 2.917 Å.[12]

Fluorescence Intensity of Adpa Complexes. The fluorescence spectra of 1:1 M(II)/adpa complexes studied here are seen in Figure 7a and b. It is seen that the usual order

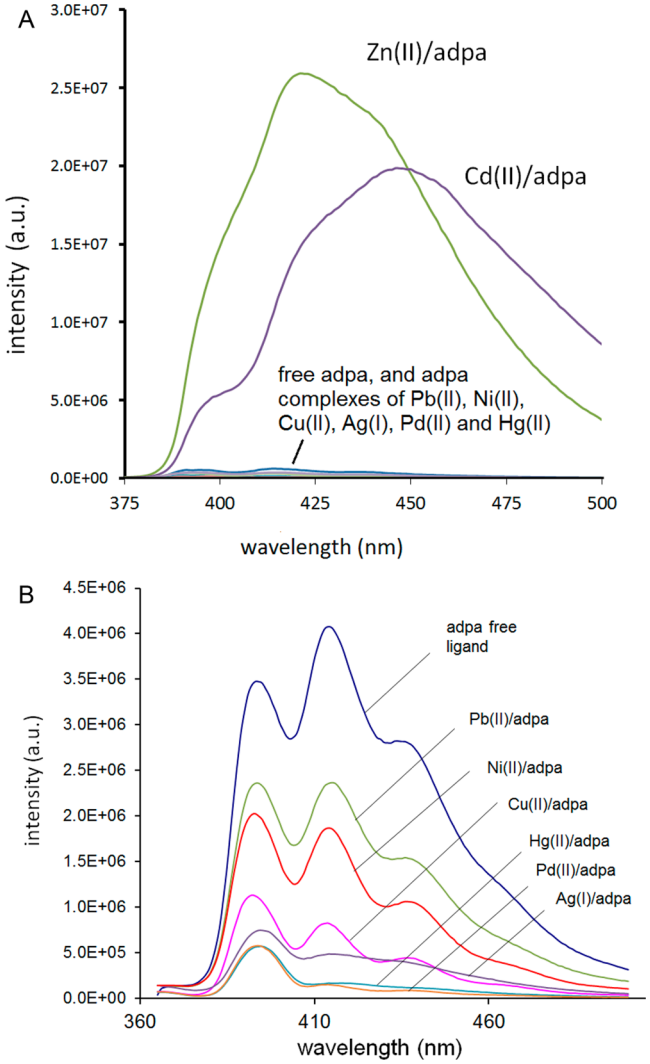

Figure 7. (a) Fluorescence spectrum of free adpa (pH 6.4, 5×10^{-6} M), plus fluorescence spectra of adpa complexes indicated (5×10^{-6} M), all in 50% MeOH/H_2O. Note that the slit setting on the instrument here is 2, to prevent a too intense spectrum, where the slit setting for Figure 7b was 5. Excitation wavelength = 350 nm. (b) Fluorescence spectra of the free adpa ligand (5×10^{-6} M), and the more weakly fluorescing adpa complexes in Figure 7a of the metal ions indicated (5×10^{-6} M), all in 50% MeOH/H_2O, pH 6.4. Note that the slit setting on the instrument here is 5, to produce more intense spectra, where the slit setting for Figure 7a was 2. Excitation wavelength = 350 nm.

of intensity of fluorescence of the complexes is observed, namely, Zn(II) > Cd(II) ≫ Pb(II) ~ Ni(II) ~ Ag(I) ~ Cu(II) ~ Pd(II) ~ Hg(II). The Zn(II) ion, which does not form a π contact with the anthracenyl fluorophore of adpa, as seen in Figure 5, shows the most intense fluorescence, followed by the Cd(II) adpa complex. The lower fluorescence intensity for the Cd(II) complex may reflect a mixture in solution of π contacted (weakly fluorescent) and non-π contacted (fluorescent) forms.[15] The remaining metal ions all decreased fluorescence intensity in their adpa complexes: it is these same metal ions that all (except for Cu(II)) show π contacts with the

dx.doi.org/10.1021/ic5008632 | Inorg. Chem. 2014, 53, 9014−9026

anthracenyl fluorophore in their adpa complexes, supporting the idea that it is the formation of π contacts that leads to quenching of fluorescence in complexes of diamagnetic metal ions with tethered fluorophores. These conclusions have been supported by TDDFT calculations.[12] Cu(II) has a strong tendency to form π contacts, as seen in the large number of π contacts for Cu(II) in Table 7, and does so with a variety of dpya based sensors: the CSD[16] yields 42 structures of Cu(II) complexes with DPA based ligands where there is a π contact with an attached aromatic group. The two reported structures of the Cu(II)/adpa complex[12,17] resemble the Zn(II)/adpa complex in **4**, in having the anthracenyl fluorophore rotated away from the Cu(II), with no π contact present.

Factors That Control π Contacts. One sees in Table 7 that for a wide selection of metal ions, M···C π contacts are quite common. One should note, however, that for many metal ions such as Ca(II) or La(III), such contacts are limited to organometallic type compounds with low coordination numbers and are not present in coordination complexes that might have a bearing on the formation of π contacts in sensors such as adpa. Metal ions that form primarily π complexes of an organometallic type are indicated in Table 7 by an asterisk. In searching the CSD[16] and drawing up Table 7, the very large number of M···C contacts shorter than the sum of the van der Waals radii produced by coordinated aromatics with M−C bonds, or pyridyl groups bonded through N, had to be excluded (Scheme 2). Also excluded were short M···C contacts produced by ligands where an aromatic group was attached directly to a coordinated donor atom, as in phenols. Many metal ions, particularly alkali metal ions and metal ions such as Ag(I), produce many short contacts with aromatic groups that are side-on or off to one side of the aromatic group at very shallow angles with the plane of the aromatic ring. Since our interest here is in π contacts similar to those found in the adpa complexes, where the metal lies above the aromatic ring, such "side-on" structures were excluded by requiring at least three M···C contacts with carbons (what might be regarded as a η^3 contact) of the aromatic ring that were shorter than the sum of the van der Waals radii (structure 'd' in Scheme 2). (The nature of such side-on nonbonded contacts is presently being explored by DFT calculation.) Requiring three short M···C contacts leads to placement of the metal ion over the ring and excludes structures where the metal ion is placed to one side of the ring with a shallow angle between the M···C contact and the plane of the ring. For Pd(II) and Pt(II) in particular, but also for other metal ions, there were a large number of structures where the metal ion was above but a little to one side of the aromatic ring (resembling structure 'e' in Scheme 2), and these were counted by allowing for a short central M···C contact, but with two adjacent M···C contacts that were up to 0.5 Å longer than the sum of the van der Waals radii. Such structures in fact resemble quite closely the π contacted M(II)/adpa structures reported here and elsewhere.[12,15] In these adpa structures, the M···C···C angle involving two aromatic C atoms *para* to each other, where the first C atom makes the short π contact, are for the metal ions so far studied: Pb(II), 108.7°; Pd(II), 112.4°; Ag(I), 107.9°; Cd(II), 114.1°; Hg(II), 113.1° (all with coordinated NO_3^- anions, except for Hg(II)[12] which has Cl^-).

Table 7 suggests that what possibly controls the ability of metal ions to form numerous π contacts in solution is the ease of desolvation of the metal ion at the potential point of formation of the π contact. In the solid state, the requirement would be displacement of coordinated anions or solvent molecules by formation of the π contact. Types of metal ions that fit this idea are (1) alkali metal ions such as Na(I), K(I), or Cs(I); (2) d^{10} metal ions such as Ag(I) or Hg(II); (3) metal ions with an "inert pair" of electrons such as Tl(I), Bi(III), or Pb(II); (4) square planar or tetragonal metal ions such as Cu(II) or Pd(II) where a π contact can form on the vacant or easily desolvated axial site.

Many metal ions not fitting into the four groups above form more than a few structures showing π contacts, such as Ca(II) or La(III), but it is not clear that these have any bearing on whether these metal ions would form π contacts with fluorophores in aqueous solution. Thus, the 39 structures found[16] where there is a Ca···C π contact, all involve organometallic type complexes with such features as low coordination numbers and Ca−C or Ca−P σ bonds that would not survive in aqueous solution or any polar solvent. The 34 structures for La(III) are similar, with η^5 cyclopentadienyl ligands rather common, in addition to the La···C π contacts to aromatic rings, which are frequently η^6.

Not considered here either are organometallic complexes such as the 1189 structures of Cr(0) where aromatic rings are coordinated in an η^6 fashion with short Cr−C bonds that are on the order of 2.25 Å. The interest is in the long M···C π contacts that appear able to form in solution, as seen here for adpa complexes, and that appear able to quench fluorescence. One suggests that the Pb(II) ion forms a π contact near the proposed site of the lone pair in the Pb(II)/adpa structure (**1**) because the bonds near the lone pair are weak, and it is at this point that desolvation to allow for the formation of the Pb···C contact is most favorable. In fact, our DFT calculations indicate that the covalency of Pb···C interaction is much weaker than that of Hg···C interaction. Bond order (BO) analyses showed that the average BO for metal−N interaction is similar for Pb/ADPA and Hg/ADPA complexes, 0.306 and 0.344, respectively. However, there is a significant difference in the strength of M···C interaction between two complexes. The BO(Pb−C) is 0.053, which is only 17% of the average BO(Pb−N) in the Pb/ADPA$(H_2O)_2$ complex, whereas the BO(Hg−C) is 0.155, 45% of the BO(Hg−N). Therefore, a Pb···C π contact near the lone pair would be less covalent, and might account for the lesser ability of the Pb(II) ion to quench the fluorescence of adpa, as seen in Figure 7b.

Disruption of Cd···C π Contacts As the Basis for Fluorescent Anion Sensors. It was previously reported[15] that in the presence of added Cl^- ion, the fluorescence intensity of the Cd(II)/adpa complex increased strongly. It was suggested that the mechanism of this was weakening or disruption of fluorescence-quenching π contacts by coordina-

Scheme 2. Considerations in Searching the CSD[16] for Structures That Have Metals π Contacted with Aromatic Rings

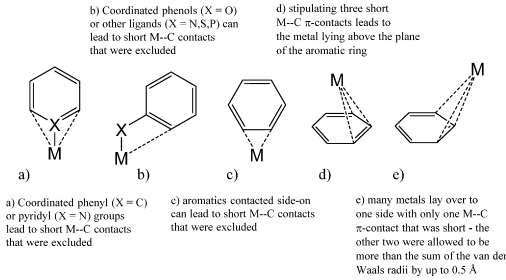

dx.doi.org/10.1021/ic5008632 | Inorg. Chem. 2014, 53, 9014−9026

tion of Cl^- ions. Figure 8 shows the effect of added $S_2O_3^{2-}$ on the fluorescence intensity of a 5×10^{-6} M solution of adpa,

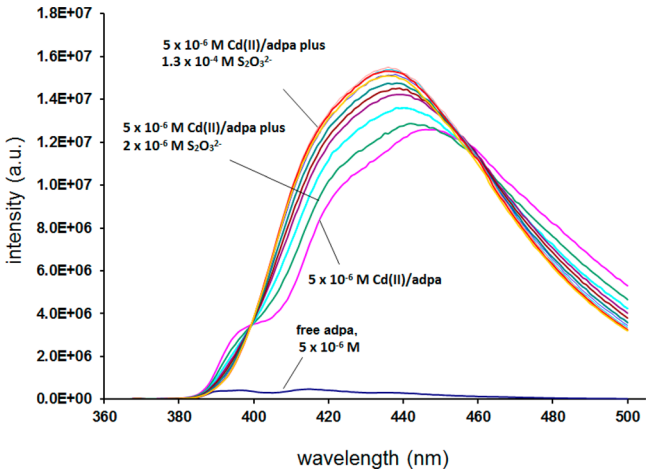

Figure 8. Effect of added $S_2O_3^{2-}$ (as $Na_2S_2O_3$) on the fluorescence spectrum of 5×10^{-6} M Cd(II)/adpa complex in 50% MeOH/H_2O at 25 °C. Excitation wavelength = 350 nm.

with 5×10^5 M Cd^{2+} present to completely form 5×10^{-6} M Cd(II)/adpa complex. It is seen that there is a considerable increase in fluorescence intensity as the concentration of $S_2O_3^{2-}$ increases. Similar results are obtained for SCN^- and Br^- (Figure 9). SO_4^{2-} has little effect on the fluorescence spectrum

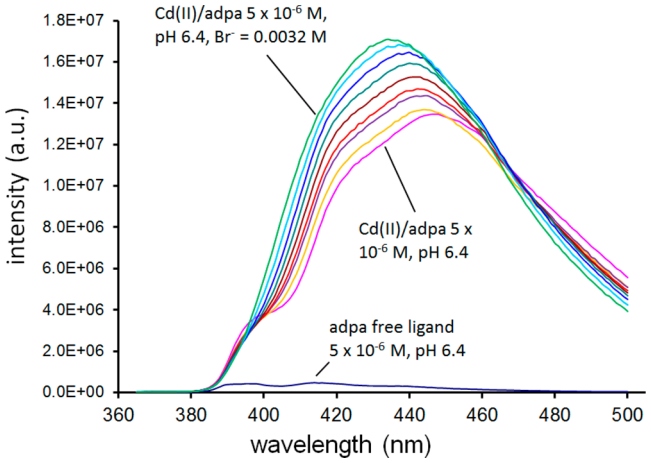

Figure 9. Effect of added Br^- (as NaBr) on the fluorescence spectrum of 5×10^{-6} M Cd(II)/adpa complex in 50% MeOH/H_2O at 25 °C. Excitation wavelength = 350 nm.

of the Cd(II)/adpa complex, suggesting that in the $S_2O_3^{2-}$ titration, an $S_2O_3^{2-}$ bonded to the Cd(II) ion in its adpa complex through S disrupts the Cd···C π contact to the fluorophore. An intriguing aspect of Figures 8 and 9 is that as either $S_2O_3^{2-}$ or Br^- binds to the Cd(II)/adpa complex, the emission band shifts and increases in intensity, and comes to resemble the emission spectrum of Zn(II)/adpa in Figure 7a. This is exactly what one would expect if coordination of $S_2O_3^{2-}$ or Br^- to Cd(II)/adpa caused the equilibrium to shift so that only the weakly π contacted or non-π contacted form of the complex was present, resembling the Zn(II)/adpa complex, where crystallography suggests that no π contact is present.

One may use the variation of fluorescence intensity with added ligand concentration to calculate log K values for the binding of Cl^-, Br^-, SCN^-, and $S_2O_3^{2-}$ to the Cd(II)/adpa complex (Table 8). These log K values are effectively at ionic

Table 8. Formation Constants for the Binding of Some Anions to the Cd(II)/adpa Complex in 50% MeOH/H_2O at 25 °C[a]

anion	equilibrium	log K	log K_1 (Cd^{2+}(aq))
Cl^-	$Cd(adpa)^{2+} + Cl^- \leftrightarrows Cd(adpa)Cl^+$	2.9	1.98
Br^-	$Cd(adpa)^{2+} + Br^- \leftrightarrows Cd(adpa)Br^+$	3.4	2.15
I^-	$Cd(adpa)^{2+} + I^- \leftrightarrows Cd(adpa)I^+$	4.5	2.28
SCN^-	$Cd(adpa)^{2+} + SCN^- \leftrightarrows Cd(adpa)SCN^+$	2.3	1.93
$S_2O_3^{2-}$	$Cd(adpa)^{2+} + S_2O_3^{2-} \leftrightarrows Cd(adpa)S_2O_3$	5.3	3.92

[a]The constants were determined from the variation of fluorescence intensity as a function of concentration of added anion, as described in the text. Because of the low concentrations of all the species in these equilibria ($\leq 10^{-3}$ M), the reported constants are effectively at ionic strength (μ) zero. The log K_1 values[50] for the same anions with the Cd^{2+}(aq) ion in aqueous solution at $\mu = 0$ and 25 °C are included for comparison.

strength (μ) zero, because the concentrations of all ionic species present do not exceed 10^{-3} M; the addition of electrolytes to achieve an ionic strength of, for example, 0.1 M, was avoided as these low-solubility ligands have been found to be salted out of solution by such electrolytes. Also shown for comparison in Table 8 are log K_1 values[50] for binding of the same ligands to the Cd^{2+}(aq) ion in aqueous solution at $\mu = 0$. It is seen that the log K_1 values for binding of unidentate ligands to the Cd(II)/adpa complex in 50% MeOH/H_2O are uniformly higher than log K_1 for the same ligands binding to the Cd^{2+}(aq) in water. This difference in log K_1 values may be due to the different solvents and may also reflect a more covalent binding tendency of Cd(II) in its adpa complex. Of particular interest is the uniquely high log K_1 for binding of I^- to the Cd(II)/adpa complex. Unlike Cl^- and Br^-, I^- produces a powerful quenching of the fluorescence of the Cd(II)/adpa complex, far more than is produced by I^- in quenching the fluorescence of the Zn(II)/adpa complex, which appears to be only collisional quenching. It seems possible that the I^- bound to the Cd(II)/adpa complex forms π contacts with the fluorophore, stabilizing the resulting complex, and leading to enhanced quenching. This possibility is being explored by attempts to grow crystals of [Cd(adpa)I_2] and by DFT calculations.

DFT Calculations on the Strengths of π Contact Formation in adpa Complexes. The question of the energetics of formation of π contacts in M(II)/adpa complexes was investigated by calculating ΔE for the overall reaction:

$$[M(adpa)(H_2O)_3]^{2+}(g)\ (\text{no } \pi \text{ contact}) \rightarrow [M(adpa)(H_2O)_2]^{2+}(g)\ (\text{with } \pi \text{ contact}) + H_2O(g) \quad (1)$$

The results in Table 9 show that for all the M(II)/adpa complexes in the gas phase, for the reaction where a coordinated water molecule is removed from the metal ion, and replaced by the formation of a π contact with the anthracenyl fluorophore, ΔE is energetically unfavorable. This

dx.doi.org/10.1021/ic5008632 | Inorg. Chem. 2014, 53, 9014−9026

Table 9. Energies (ΔE) Calculated by DFT as Described in the Text, for the Gas-Phase Reaction $[M(adpa)(H_2O)_3]^{2+}(g)$ (with no π contact) → $[M(adpa)(H_2O)_2]^{2+}(g)$ (with π Contact) + H_2O (g)

M =	Ca(II)	Zn(II)	Cd(II)	Hg(II)	Pb(II)
ΔE^a	15.61	15.71	14.68	11.86	9.88

[a] In kcal mol^{-1}.

reflects the fact that the calculations refer to the gas phase and omit the energy obtained for the displaced water being solvated by the bulk solvent in solution. However, the trend in the ΔE values is instructive. For Zn(II) and Ca(II), which are not expected to form π contacts because they produce increased fluorescence intensity with adpa, ΔE is considerably more unfavorable than for the Hg(II) and Pb(II) adpa complexes, which strongly quench fluorescence, as proposed here, by the formation of π contacts with adpa in solution. The energy for eq 1 is intermediate for Cd(II), in line with the idea that Cd(II)/adpa may exist in aqueous solution as an equilibrium mixture of the π contacted (weakly fluorescent) and non-π contacted (strongly fluorescent) forms.

Conclusions. This work has shown crystallographically that the metal ions in the Pb(II), Ag(I), and Pd(II) adpa complexes form π contacts with the anthracenyl fluorophore of adpa, in line with previous results[12] showing that the Hg(II) also forms π contacts in its adpa complexes. These same metal ions all strongly quench the fluorescence of adpa. In contrast, the Zn(II) does not form a π contact in its adpa complex and shows a strong greatly enhanced fluorescence with adpa. Cu(II)/adpa shows very strong quenching of fluorescence, in spite of the two reported crystal structures for the complex showing no Cu···C π contact. This may simply be that the mechanism of quenching by paramagnetic ions such as Cu(II) occurs via a redox mechanism that does not require π contacts. However, a survey of M···C π contacts in the CSD[16] shows that Cu(II) forms a large number of π contacts in its complexes, and it may be that Cu(II) has even short-lived π contacts in solution that are not essential to but enhance the proposed redox quenching mechanism. The survey of M···C π contacts[16] showed that the greatest tendency to form such π contacts occurred with (1) metal ions such as Pb(II), Sn(II), Bi(III), Sb(III), and Tl(I), that have an "inert" pair of electrons, and weak M−L bonding near the inert pair that enables displacement of a coordinated water to form a π contact, (2) d^{10} metal ions such as Ag(I) and Hg(II), that have "linear" coordination geometry involving short covalent bonds, with long weak bonds at right angles to these, where desolvation may more easily take place to allow for the formation of π contacts, (3) square planar or tetragonally distorted metal ions such as Cu(II), Pd(II), or Pt(II), where any axial solvent molecules are easily displaced to allow for the formation of π contacts, and (4) alkali metal ions such as Na(I) and K(I), which also are weakly solvated, so allowing for easy displacement of coordinated solvent molecules so as to allow for formation of π contacts.

The Cd(II)/adpa complex shows less intense fluorescence than Zn(II)/adpa.[21] It has been proposed[15] that Cd(II)/adpa may exist in aqueous solution as an equilibrium mixture of the π contacted (weakly fluorescent) and non-π contacted (strongly fluorescent) forms. This proposal leads to the possibility that the π contacts in Cd(II)/adpa can be disrupted by coordination of simple ligands, increasing fluorescence intensity, and allowing for use of complexes such as Cd(II)/adpa as small molecule or anion sensors. This is demonstrated to be the case for Cl^-, Br^-, SCN^-, and $S_2O_3^{2-}$. The crystal structure of $[Cd(adpa)Br_2]$ (**5**) shows a considerably lengthened Cd···C π contact of 3.369 Å, as compared to 3.018 Å in $[Cd(adpa)(NO_3)_2]$.[15] The trend appears to be that coordination of more covalently binding ligands such as Cl^- to the Cd(II)/adpa lengthens the Cd···C π contacts, which may be sufficient to restore fluorescence. The variation of the fluorescence intensity of the Cd(II)/adpa complex with concentration of added anions allows for the calculation of log K values for the Cl^-, Br^-, I^-, SCN^-, and $S_2O_3^{2-}$ complexes, which fall in the range log K equals 3 to 6. The phenomenon of enhanced fluorescence intensity for the Cd(II)/adpa complexes on coordination of the above anions may form the basis of a new type of anion or small molecule sensor.

DFT calculations show that the energy of displacement of a coordinated water molecule and formation of a π contact in the Ca(II) and Zn(II) adpa complexes is least favorable, while for the Pb(II) and Hg(II) complexes it is the most favorable, in line with the tendencies of the latter metal ions to form π contacts. Cd(II) in its adpa complex appears to be intermediate, in line with its proposed tendency to form weaker π contacts, only partly formed in aqueous solution.

This work has suggested that in the case of adpa with its anthracenyl fluorophore, M···C π contacts between heavy metal ions such as Hg(II), Pd(II), Ag(I), and Pb(II) and the fluorophore are responsible for quenching fluorescence. Future work will attempt to establish whether such π contacts are generally responsible for quenching fluorescence with tethered fluorophores by studying ligands with other fluorophores such as coumarin (cdpa in Figure 1) or indole based groups (idpa). An important question is whether the Cd(II) complexes with such fluorophores would also act as potential anion/small molecule sensors. An important sensor design strategy for heavy metals such as Hg(II) will be to design ligands where the formation of π contacts will be hindered, so as to produce deliberately designed fluorescent sensors. An interesting example of such a sensor is seen with a Hg(II) complex where there are four fluorophores.[51] A PET effect in the unbound ligand means that the latter fluoresces only weakly. However, the addition of Hg(II) shows a strong increase in fluorescence. A crystal structure shows that only two of the fluorophores are involved in π contacts with the Hg(II): this means that the two non-π contacted fluorophores directed well away from the Hg(II) are able to fluoresce strongly.

An important aspect of using crystallography to analyze PET sensors is to show that the proposed π contacts are present in solution. In the case of cyclen-based ligands for enhanced complexation of Ag(I) due to the formation of π contacts with anthracenyl and naphthyl groups, Habata et al.[52] have demonstrated the presence of such π contacts crystallographically and also shown from 2D ^{1}H NMR that π contacts with the same C atoms as in the solid state are present in solution. It has also been found crystallographically by Elliott et al.[53] that coordination of K^+ to diaza-crowns with fluorophores attached to the N donors of the crown, leads to π contacts between the fluorophores and the K^+. It was tentatively suggested that the π contacts found between the K^+ and the fluorophores of the ligands may have led to the quenching of the sensors observed in solution. It is also possible that K^+ quenches the fluorescence of the latter ligands because the K−N bonds formed are insufficiently covalent to lower the energy

dx.doi.org/10.1021/ic5008632 | Inorg. Chem. 2014, 53, 9014−9026

of the lone pair on the N donor, and so a PET effect occurs. From a theoretical standpoint, more DFT calculations are in progress in our group to examine the mechanism whereby metal-fluorophore π contacts cause quenching of fluorescence, with particular attention paid to the role of covalence in both the M···C π contacts and the M−N bond.

■ ASSOCIATED CONTENT

Supporting Information

Crystallographic information files. This material is available free of charge via the Internet at http://pubs.acs.org.

■ AUTHOR INFORMATION

Corresponding Author

*E-mail: hancockr@uncw.edu.

Notes

The authors declare no competing financial interest.

■ ACKNOWLEDGMENTS

The authors thank the University of North Carolina, Wilmington, for a research assistantship to J.W.N. Dr. Ralph N. Mead is thanked for assistance with mass spectrometry, and the NSF Division of Chemistry is thanked for providing the mass spectrometer used under grant CHE1039784.

■ REFERENCES

(1) Wenzel, M.; Hiscock, J. R.; Gale, P. A. *Chem. Soc. Rev.* **2012**, *41*, 480.
(2) Beer, P. D.; Gale, P. A. *Angew. Chem., Int. Ed.* **2001**, *40*, 486.
(3) Bencini, A.; Bernardo, M. A.; Bianchi, A.; Garcia-Espana, E.; Giorgi, C.; Luis, S.; Pina, F.; Valtancoli, B. *Adv. Supramol. Chem.* **2002**, *8*, 79.
(4) (a) Hilderbrand, S. A.; Lim, M. H.; Lippard, S. J. *Top. Fluoresc. Spectrosc.* **2005**, *9*, 163. (b) Kim, H. N.; Ren, W. X.; Kim, J. S.; Yoon, J. *Chem. Soc. Rev.* **2012**, *41*, 3210. (c) Lodeiro, C.; Capelo, J. L.; Mejuto, J. C.; Oliveira, E.; Santos, H. M.; Pedras, B.; Nuñez, C. *Chem. Soc. Rev.* **2010**, *39*, 2948. (d) Xu, Z.; Yoon, J.; Spring, D. R. *Chem. Soc. Rev.* **2010**, *39*, 1996. (d) Bernard, B.; Leray, I. *Coord. Chem. Rev.* **2000**, *205*, 3.
(5) Thompson, R. B.; Bozym, R. A.; Cramer, M. L.; Stoddard, A. K.; Westerberg, N. M.; Fierke, C. A. *Fluoresc. Sens. Biosens.* **2006**, 107.
(6) Parker, D.; Williams, J. A. G. *Metal Ions Biol. Syst.* **2003**, *40*, 233.
(7) Burdette, S. C.; Lippard, S. J. *Coord. Chem. Rev.* **2001**, *216*, 333.
(8) (a) Wiosna, G.; Petkova, I.; Mudadu, M. S.; Thummel, R. P.; Waluk, J. *Chem. Phys. Lett.* **2004**, *400*, 379. (b) Waluk, J. *Acc. Chem. Res.* **2003**, *36*, 832.
(9) Czarnik, A. *Trends Org. Chem.* **1993**, *4*, 123.
(10) de Silva, A. P.; Gunaratne, H. Q. N.; Gunnlaugsson, T.; Huxley, A. J. M.; McCoy, C. P.; Rademacher, J. T.; Rice, T. E. *Chem. Rev.* **1997**, *97*, 1515.
(11) Williams, N. J.; Dean, N. E.; VanDerveer, D. G.; Luckay, R. C.; Hancock, R. D. *Inorg. Chem.* **2009**, *48*, 7853.
(12) (a) Lee, H.; Lee, H.-S.; Reibenspies, J. H.; Hancock, R. D. *Inorg. Chem.* **2012**, *51*, 10904. (b) Lee, H.; Hancock, R. D.; Lee, H.-S. *J. Phys. Chem. A* **2013**, *117*, 13345.
(13) Gan, W.; Jones, S. B.; Reibenspies, J. H.; Hancock, R. D. *Inorg. Chim. Acta* **2005**, *358*, 3958.
(14) Zalewski, P. D.; Forbes, I. J.; Betts, W. H. *Biochem. J.* **1993**, *296*, 403.
(15) Nugent, J. W.; Lee, H.; Lee, H.-S.; Reibenspies, J. H.; Hancock, R. D. *Chem. Commun.* **2013**, *49*, 9749.
(16) *Cambridge Structural Database*; Cambridge Crystallographic Data Centre: Cambridge, U. K., 2013.
(17) (a) Gokel, G. W.; Barbour, L. J.; De Wall, S. L.; Meadows, E. S. *Coord. Chem. Rev.* **2001**, *222*, 127. (b) Petrella, A. J.; Raston, C. L. *J. Organomet. Chem.* **2004**, *689*, 4125. (c) Ma, J. C.; Dougherty, D. A. *Chem. Rev.* **1997**, *97*, 1303. (d) Yi, H.-B.; Lee, H. M.; Kim, K. S. *J. Chem. Theory Comput.* **2009**, *5*, 1709. (e) Gokel, G. W. *Int. Congr. Ser.* **2007**, *1304*, 1. (f) Andrews, L. J. *Chem. Rev.* **1954**, *54*, 713. (g) Kim, S. K.; Vargas-Zuniga, G. L.; Hay, B. P.; Young, N. J.; Delmau, L. H.; Masselin, C.; Lee, C.-H.; Kim, J. S.; Lynch, V. M.; Moyer, B. A.; Sessler, J. L. *J. Am. Chem. Soc.* **2012**, *134*, 1782.
(18) Antonioli, B.; Buchner, B.; Clegg, J. K.; Gloe, K.; Gloe, K.; Gotzke, L.; Heine, A.; Jager, A.; Jolliffe, K. A.; Kataeva, O.; Kataev, V.; Klingeler, R.; Krause, T.; Lindoy, L. F.; Popa, A.; Seichter, W.; Wenzel, M. *Dalton Trans.* **2009**, 4795.
(19) Kim, M. J.; Swamy, K. M. K.; Lee, K. M.; Jagdale, A. R.; Kim, Y.; Kim, S.-J.; Yoo, K. H.; Yoon, J. *Chem. Commun.* **2009**, 7215.
(20) Hancock, R. D. *Chem. Soc. Rev.* **2013**, *42*, 1500.
(21) Ojida, A.; Mito-Oka, Y.; Inoue, M.; Hamachi, I. *J. Am. Chem. Soc.* **2002**, *124*, 6256.
(22) Hedges, J. I.; Stern, J. H. *Limnol. Oceanogr.* **1984**, *29*, 663.
(23) Gabe, E. J.; Le Page, Y.; Charland, J.-P.; Lee, F. L.; White, P. S. *J. Appl. Crystallogr.* **1989**, *22*, 384.
(24) *FluorEssence program*, version 2.1; HORIBA Jobin Yvon, Inc.: Edison, NJ, 2006.
(25) Schmidt, M. W.; Baldridge, K. K.; Boatz, J. A.; Elbert, S. T.; Gordon, M. S.; Jensen, J. H.; Koseki, S.; Matsunaga, N.; Nguyen, K. A.; Su, S.; Windus, T. L.; Dupuis, M.; Montgomery, J. A. *J. Comput. Chem.* **1993**, *14*, 1347.
(26) Lee, C.; Yang, W.; Parr, R. G. *Phys. Rev. B* **1988**, *37*, 785.
(27) Becke, A. D. *J. Chem. Phys.* **1993**, *98*, 5648.
(28) Weigend, F.; Ahlrichs, R. *Phys. Chem. Chem. Phys.* **2005**, *7*, 3297.
(29) Hay, P. J.; Wadt, W. R. *J. Chem. Phys.* **1985**, *82*, 270.
(30) Hay, P. J.; Wadt, W. R. *J. Chem. Phys.* **1985**, *82*, 284.
(31) Hay, P. J.; Wadt, W. R. *J. Chem. Phys.* **1985**, *82*, 299.
(32) ORTEP-3 for Windows, version 1.08: Farrugia, L. J. *J. Appl. Crystallogr.* **1997**, *30*, 565.
(33) Lawton, S. L.; Kokatailo, G. T. *Inorg. Chem.* **1972**, *11*, 363.
(34) Shimoni-Livny, L.; Glusker, J. P.; Bock, C. W. *Inorg. Chem.* **1998**, *37*, 1853.
(35) Hancock, R. D.; Shaikjee, M. S.; Dobson, S. M.; Boeyens, J. C. A. *Inorg. Chim. Acta* **1988**, *154*, 229.
(36) Hancock, R. D.; Reibenspies, J. H.; Maumela, H. *Inorg. Chem.* **2004**, *43*, 298.
(37) Luckay, R.; Cukrowski, I.; Mashishi, J.; Reibenspies, J. H.; Bond, A. H.; Rogers, R. D.; Hancock, R. D. *J. Chem. Soc., Dalton Trans.* **1997**, 90.
(38) Cordero, B.; Gómez, V.; Platero-Prats, A. E.; Revés, M.; Echeverría, J.; Cremades, E.; Barragán, F.; Alvarez, S. *Dalton Trans.* **2008**, *21*, 2832.
(39) Greenwood, N. N.; Earnshaw, A. *Chemistry of the Elements*, 2nd ed., Butterworth: Oxford U. K., 2001; p 1218.
(40) Andrews, L. J.; Keefer, R. M. *J. Am. Chem. Soc.* **1949**, *71*, 3644.
(41) Bondi, A. *J. Phys. Chem.* **1964**, *68*, 441.
(42) Pyykkö, P. *Chem. Rev.* **1997**, *97*, 597.
(43) Kuto, K.; Mori, A. *J. Mater. Chem.* **2005**, *15*, 2902.
(44) Al Shihadeh, Y.; Benito, A.; Lloris, J. M.; Martinez-Manez, R.; Pardo, T.; Soto, J.; Marcos, M. D. *J. Chem. Soc., Dalton Trans.* **2000**, 1199.
(45) Sancenon, F.; Benito, A.; Hernandez, F. J.; Lloris, J. M.; Martınez Manez, R.; Pardo, T.; Soto, J. *Eur. J. Inorg. Chem.* **2002**, 866.
(46) Aragoni, M. C.; Arca, M.; Bencini, M.; Blake, A. J.; Caltagirone, C.; Danesi, A.; Devillanova, F. A.; Garau, A.; Gelbrich, T.; Isaia, F.; Lippolis, V.; Hursthouse, M. B.; Valtancoli, B.; Wilson, C. *Inorg. Chem.* **2007**, *46*, 8088.
(47) Mikata, Y.; Wakamatsu, W.; Kawamura, A.; Yamanaka, N.; Yano, S.; Odani, A.; Morihiro, K.; Tamotsu, S. *Inorg. Chem.* **2006**, *45*, 9262.
(48) Bazzicalupi, C.; Bencini, A.; Bianchi, A.; Giorgi, C.; Fusi, V.; Valtancoli, B.; Bernado, M. A.; Pina, F. *Inorg. Chem.* **1999**, *38*, 3806.
(49) Cockrell, G. M.; Zhang, G.; VanDerveer, D. G.; Thummel, R. P.; Hancock, R. D. *J. Am. Chem. Soc.* **2008**, *130*, 1420.
(50) Martell, A. E.; Smith, R. M. *Critical Stability Constant Database*; National Institute of Science and Technology (NIST): Gaithersburg, MD, 2003; Vol. *46*.

(51) Li, H. W.; Li, Y.; Dang, Y.-Q.; Ma, L.-J.; Wu, Y.; Hou, G.; Wu, L. *Chem. Commun.* **2009**, 4453.
(52) Habata, Y.; Oyama, Y.; Ikeda, M.; Kuwahara, S. *Dalton Trans.* **2013**, *42*, 8212.
(53) Elliott, E. K.; Hu, J.; Gokel, G. W. *Supramol. Chem.* **2007**, *19*, 175.

dx.doi.org/10.1021/ic5008632 | *Inorg. Chem.* 2014, 53, 9014−9026